Published in final edited form as:
Nanoscale. 2013 May 7; 5(9): 3904–3911. doi:10.1039/c3nr90022c.

Development of drug loaded nanoparticles for tumor targeting. Part 2: enhancement of tumor penetration through receptor mediated transcytosis in 3D tumor models

Mohammad H. El-Dakdouki[a,c], **Ellen Puré**[b], and **Xuefei Huang**[a,*]

[a]Department of Chemistry, Chemistry Building, Room 426, 578 S. Shaw Lane, Michigan State University, East Lansing, MI 48824, USA

[b]The Wistar Institute, Room 372, 3601 Spruce Street, Philadelphia, PA 19104, USA

Abstract

We report that receptor mediated transcytosis can be utilized to facilitate tumor penetration by drug loaded nanoparticles (NPs). We synthesized hyaluronan (HA) coated silica nanoparticles (SNPs) containing a highly fluorescent core to target CD44 expressed on cancer cell surface. Although prior studies have primarily focused on CD44 mediated endocytosis to facilitate cellular uptake of HA-NPs by cancer cells, we discovered that once internalized, the HA-SNPs could be transported out of the cells with its cargo. The exported NPs could be taken up by neighboring cells. This enabled the HA-SNPs to penetrate deeper inside tumor and reach much greater number of tumor cells in 3D tumor models, presumably through tandem cycles of CD44 mediated endocytosis and exocytosis. When doxorubicin (DOX) was loaded onto the NPs, better penetration of multilayered tumor cells was observed with much improved cytotoxicites against both drug sensitive and drug resistant cancer spheroids compared to free drug. Thus, targeting receptors such as CD44 that can readily undergo recycling between cell surface and interior of the cells can become a useful strategy to enhance tumor penetration potential of NPs and the efficiency of drug delivery through receptor mediated transcytosis.

Keywords

cancer spheroids; CD44; hyaluronan; tissue penetration; transcytosis

1. Introduction

Poor intratumoral drug penetration and distribution is gaining much attention in recent years as a key factor in drug resistance during chemotherapy of cancer.[1, 2] Although nanoscaled constructs have been developed to enhance local concentrations of drugs in tumors through the enhanced retention and permeability (EPR) effect, the ability of the chemotherapeutic drugs to penetrate deep in the tumor is still limited. Several innovative strategies have been investigated to improve NP/drug penetration, including co-administration of a tumor penetrating peptide,[3, 4] incorporation of extracellular matrix modifying enzymes in the formulation,[5] magnet assisted penetration,[6] and reduction of NP diameters.[7–9] Herein, we

Tel: +1-517-355-9715, ext 329, Fax: +1-517-353-1793, xuefei@chemistry.msu.edu.
[c]Current address: Department of Chemistry, Beirut Arab University, Beirut, Lebanon.

Supporting Information

Electronic supplementary information (ESI) available: detailed experimental procedures on spheroid preparation, SEM sample processing, NPs uptake by flow cytometry, and supporting figures and tables. See DOI: #####.

describe a new approach utilizing the transcytosis process mediated by a cell surface receptor, i.e., CD44, to enhance NP penetration of tumor. In the preceding paper,[10] we reported the synthesis and characterization of HA-SNPs and demonstrated that the HA coating on fluorescent SNPs significantly enhanced the uptake of the NPs by SKOV-3 ovarian cancer cells mainly through CD44 mediated endocytosis. In this manuscript, we describe the finding that HA-SNPs internalized by cancer cells can be exocytosed. The combined CD44 endocytosis and exocytosis processes (also referred to as transcytosis) enable cellular penetrations by HA-SNPs, allowing their delivery deep inside the tumor and enhancing the efficiency of DOX in killing the cancer cells in 3D tumor models.

2. Materials and Methods

2.1. Materials and instrumentation

All chemical were reagent grade and were used as received from the manufacturers. Bovine serum albumin (BSA), fetal bovine serum (FBS) and sodium chloride were purchased from Sigma-Aldrich. Doxorubicin hydrochloride was purchased from Shanghai FChemicals Technology Co. SKOV-3 cell line was purchased from American Type Culture Collection (ATCC). NCI/ADR-RES cell line was a gift from Prof. Paul Erhardt (University of Toledo). Phosphate buffered saline (PBS), Dulbecco's Modified Eagle Medium (DMEM), RPMI medium 1640, fluorescein isothiocyanate (FITC), sodium pyruvate (100 mM), glutamine, Penicillin-Streptomycin (Pen Strep) mixture, propidium iodide and LIVE/DEAD® Viability/Cytotoxicity Kit for mammalian cells were purchased from Invitrogen. All cell culture growth media was supplemented with 10% inactivated FBS, 1% Pen-Strep mixture, glutamine (2 mM) and sodium pyruvate (1mM). SKOV-3 cell line was cultured in DMEM while NCI/ADR-RES cells were maintained in RPMI 1640. The MDR phenotype of NCI/ADR-RES cell line was preserved by culturing the cells in growth medium spiked with DOX (400 nM). Fluorescence activated cell sorting (FACS) experiments were conducted on a BD Vantage SE flow cytometer. Fluorescence measurements were performed on a SpectraMax® M5 Multi-mode Microplate Reader (Molecular Devices). All confocal laser microscopy images were collected on an Olympus FluoView 1000 LSM confocal microscope or a Zeiss LSM Pascal. UV-vis measurements were carried out on a UV-4001 spectrometer (Hitachi High-Technologies Co., Japan). Light microscopic images of spheroids were obtained on an Olympus CKX41 inverted light microscope. SEM images were collected on a JEOL 6400V (Japan Electron Optics Laboratories) microscope equipped with a LaB6 emitter (Noran EDS).

2.2. Assay for NP exocytosis from cancer cells

SKOV-3 cells (3×10^5 cells) were cultured in a 35 mm cell culture plate overnight at 37 °C and 5% CO_2. The supernatant was removed and the cells were washed with PBS twice. HA-SNP (60 μg/ml, 2ml) in serum free DMEM was added and the cells were incubated for 5 hours at 37 °C and 5% CO_2 after which the supernatant was removed and the cells were washed with PBS six time to ensure the complete removal of NPs from the surface of the cells. Fresh serum-free DMEM (2 ml) was added to the plate, which was incubated at 37 °C and 5% CO_2. 100 μl of the supernatant were transferred at specific time points to a black, bottom clear 96-well plate, and fluorescence was measured on a plate reader (Excitation wavelength 488 nm; Emission wavelength 520 nm). The drawn samples were returned to the plate to maintain constant volume through the experiment.

2.3. Two particle assay

SKOV-3 cells (3×10^5 cells/wells) were cultured in a 6 well plate at 37 °C and 5% CO_2 overnight. The culture medium was removed, and the cells were washed with PBS. While one well received HA-SNP (FITC doped), the second one received HA-RITC-SNP

(rhodamine isothiocyanate (RITC) doped) in serum free medium. A third well did not receive any NPs and was used as the negative control. The cells were incubated at 37 °C and 5% CO_2 for 6 h after which the NP solutions were removed and the cells were washed thoroughly with PBS. The cells were collected and washed followed by trypsinization and centrifugation (2500 rpm; 4 °C). The cells were resuspended in serum containing medium. Some of the FITC- and RITC-labeled cells were mixed and transferred to one well of a 4-well plate. The other wells received unlabeled control cells, FITC-only labeled cells, or RITC-only labeled cells. Two plates were prepared and incubated at 37 °C and 5% CO_2 for 48 h. To acquire confocal microscopy images, the cells of one plate were washed with PBS, fixed with 10% neutral formalin, stained with 4',6-diamidino-2-phenylindole (DAPI), and imaged on a laser confocal microscope. To quantify the percentage of double labeled cells by flow cytometry, the cells of the second plate were washed with PBS, collected by trypsinization, resuspended in serum containing medium, transferred to FACS tubes, and analyzed on a flow cytometer.

2.4. NP transcytosis analysis using a transwell assay

SKOV-3 cells were cultured in a 100 mm cell culture plate at 37 °C and 5% CO_2 till it reached 80% confluency. Cells were trypsinized, collected by centrifugation, and resuspended in 10% FBS-DMEM to a final concentration of 8×10^5 cells/ml. Serum containing DMEM (1.5 ml) was added to the wells of a 12-well plate, above which the transwell inserts were placed. 500 μl of the cell suspension was added to each transwell (4×10^5 cells/transwell). The plate was incubated at 37 °C and 5% CO_2 for 3 weeks. The growth media was changed every 2 days during the first week, and every day during the last two weeks. The integrity of the multilayered cell culture was assessed by transendothelial electrical resistance (TEER) measurements using a Millicell-ERS Volt-Ohm Meter (Millipore). After 3 weeks, the growth media was removed and the cell layer was washed with PBS. 1.5 ml of serum free DMEM was added to the bottom of the 12-well plate wells. One transwell received HA-SNP in serum-free DMEM (0.5 ml, 0.24 mg-NP/ml), while the other received a fluorescently equivalent amount of SNP in serum-free DMEM (0.5 ml, 0.1 mg-NP/ml). 100 μl aliquots were drawn at different time points from the lower compartment, and the fluorescence was assessed on a plate reader (Excitation wavelength 488 nm; Emission wavelength 520 nm). After measurements, the aliquots were returned to its respective wells. The volume in the bottom wells was maintained at 1.5 ml. Similar protocol was used to assess the penetration of DOX and DOX-HA-SNP through the multilayered cell culture where subcytotoxic equimolar amounts of DOX were used (excitation wavelength 483 nm; emission wavelength 580 nm). For competition with free HA, transwells were incubated with HA in DMEM for 2 h after which HA-SNP was added.

2.5. Monitoring the penetration of SNPs by confocal imaging

SKOV-3 spheroids were transferred to the lid of a 100 mm cell culture plate containing 10 ml of PBS in the bottom, and washed with PBS twice. One set of spheroids received SNP in serum-free DMEM (20 μl, 0.11 mg-NP/ml), while the other received the equivalent HA-SNP (20 μl, 0.17 mg-NP/ml) based on fluorescence. The spheroids were incubated at 37 °C and 5% CO_2 for 18 h followed by washing with PBS three times. The spheroids were fixed with 10% neutral formalin (20 μl) for 30 min. The spheroids were washed twice with PBS and DI water consecutively. The spheroids were transferred to 8 well-cell culture plate where they were air dried in the dark. Z-stack images (8 μm/section) were collected on an Olympus view microscope. The same protocol was used to monitor the penetration of SNPs in NCI/ADR-RES spheroids; however, RPMI 1640 was used instead of DMEM.

2.6. Effect of DOX-HA-SNP on the morphology of spheroids: Evidence from confocal imaging and SEM

Spheroids were transferred to the lid of a 100 mm petri dish containing 10 ml of PBS. The spheroids were washed with PBS. One set was used as a negative control where spheroids were incubated with 20 μl of serum-free DMEM. A second set was incubated with HA-SNP (0.32 mg/ml, 20 μl/spheroid). The third set was incubated with DOX-HA-SNP (20 μl/spheroid, 0.32 mg-NP/ml, 1.92 μg/ml-DOX). The spheroids were incubated for 72 h at 37 °C and 5% CO_2. The spheroids were then washed thoroughly with PBS, and processed for SEM imaging (See supporting information for SEM sample processing procedures). Prior to osmium coating required for SEM imaging, fluorescence images were collected on a laser confocal microscope. The spheroids were then coated with osmium and imaged on a SEM microscope.

2.7. Trypan Blue exclusion assay for assessing spheroid viability

Eight sets of spheroids (10/set) were transferred to the lids of 100 mm cell culture plates and washed with PBS. The spheroids were treated with eight serial dilutions of DOX-HA-SNP or DOX in serum-free DMEM (20 μl/spheroid). For SKOV-3 spheroids, the concentrations of DOX_{NP} used were: 9, 4.5, 2.25, 1.125; 0.563; 0.282; 0.141; 0.071 μM, and those of free DOX were: 80, 40, 20, 10, 5, 2.5, 1.25, 0.65 μM. For NCI/ADR-RES spheroids, the concentrations of DOX_{NP} used were: 43, 21.5, 10.75, 5.38, 2.69, 1.34, 0.67, 0.34 μM, and those of free DOX were: 400, 200, 100, 50, 25, 12.5, 6.25, 3.13 μM. The spheroids were incubated with the cytotoxic reagents for 72 h. Spheroids of the same set were combined in one Eppendorf tube, centrifuged (2500rpm, 4 °C, 5 min), and dispersed using 0.25% trypsin (200 μl). Serum-containing DMEM (800 μl) was added, and the cells were centrifuged, washed and re-suspended in serum-containing DMEM (100 μl). The cells were analyzed for viability using the Trypan Blue exclusion assay. Briefly, 12 μl of cell suspension was mixed with 12 μl of 0.4% Trypan Blue/PBS. 10 μl of the mixture was loaded on a hemocytometer. The number of viable cells and total number of cells were determined. The percentage of viable cells was calculated as follows:

% viable cells= [number of viable cells/total number of cells]*100.

3. Results and discussion

3.1. Evidence for exocytosis of HA-SNP from SKOV-3 cells and evaluation of HA-SNP interactions with SKOV-3 cells in 3D culture

CD44 is known to traffic between endosomes and cell surface.[11] We envision that it is possible when CD44 is recycled to cell surface from endosomes, it can bring the bound HA species to the surface and release them to the extracellular space (exocytosis). To study the fate of HA-SNPs after cellular uptake, we developed an exocytosis assay. After the SKOV-3 cells were grown in a culture flask and incubated with HA-SNPs, the cells were washed to remove all NPs not internalized. TEM images confirmed very few particles remained on cell surface after washing (Fig. S1). Fresh cell culture medium was added to the cells and the fluorescence of cell culture supernatant was continuously monitored. Although the supernatant showed little fluorescence initially, the fluorescence intensity increased over time, which reached a plateau after 24 hours (Fig. 1a). This indicated that HA-SNPs internalized could be transported out of the cells. Quantification of the fluorescent intensity remaining inside the cells and that of the supernatant showed that 95% of the HA-SNPs were exported after 48 hours. Tirelli and coworkers reported that CD44 recycling requires tens of hours in a mouse macrophage cell line,[12] which is consistent with the rate of HA-SNP exocytosis observed in our study.

Although endocytosis of NPs has been extensively utilized for intracellular drug delivery,[13–15] comparatively, NP exocytosis has been much less studied. It has been shown that after cellular uptake, NPs such as quantum dots,[16] magnetic nanoparticles,[17] mesoporous silica particles,[18] single wall carbon nanotubes,[19] gold nanoparticles[20, 21] and polysosomes[22–24] can exit the cells. However, the exocytosis phenomenon has not been extensively explored for drug delivery applications.[25] To test whether HA-NP exocytosis can be useful for drug delivery, as the first step, we developed a two particle assay[18] to test whether the exported HA-SNPs can be taken up by another cell. The red fluorescent HA-RITC-NPs were synthesized as described for HA-SNPs except for substituting FITC-APTES with RITC-APTES. SKOV-3 cells were loaded with either the green fluorescent HA-SNPs or the red fluorescent HA-RITC-NPs in two separate culture flasks for 6 hours at 37 °C. After removing the unbound NPs by washing, the pre-loaded cells were then cultured together. Although each cell began with either green or red fluorescence, multiple cells contained both red and green fluorescence after 48 hours (Fig. 1b, Fig. S2). Quantification by flow cytometry showed a dramatic increase in the number of cells with both green and red fluorescence following the co-culture (Fig. 1c). This observation suggested that the exocytosed HA-NPs retained their abilities to be efficiently taken up by other cells.

In the traditional cell culture flask, the cells are grown as a monolayer. These 2D monolayer cell cultures do not mimic *in vivo* tumor well since extracellular barriers are not reproduced. 3D multilayered cell culture (MCC) and tumor spheroids have emerged as a powerful and promising predictive tool for chemotherapeutic evaluation.[26–28] 3D cultures can mimic the 3D cellular context and relevant pathophysiological gradients encountered in tumors *in vivo*.[26, 29] Some chemotherapeutic drugs that exhibited activities in 2D cell cultures lose potencies in 3D cultures due to the extracellular barriers encountered in 3D models.[2, 30] Therefore, we evaluated transcytosis of HA-SNPs using both MCC and spheroids of SKOV-3 cells.

Endocytosis and exocytosis were monitored on the same side of the cells in the 2D monolayer culture. To distinguish the direction of NP transport, multiple layers of SKOV-3 cells were grown on a permeable transwell filter as a model of MCC.[31] The NP solution was added to the chamber above MCC and the ability for NPs to penetrate through the MCC was assessed by monitoring the fluorescence of the chamber below MCC as a function of time. TEER measurements showed that addition of SNPs or HA-SNPs did not change the electrical resistance of the MCC through the entire assay (Table S1) suggesting that the NPs did not affect the junction dynamics of the cells. With the control SNPs, little increase in fluorescence of the bottom well was detected after 36 hours of incubation indicating the MCC had tight junctions between cells and the nonspecific leakage through the MCC was low (Fig. 2a). On the other hand, HA-SNPs were able to penetrate through the MCC as evident from the significant fluorescence increase in the bottom chamber presumably by a sequential series of endocytosis/exocytosis processes through the multiple layers of cells. The addition of excess free HA polymer onto the MCC prior to incubation with HA-SNPs significantly reduced the amount of NPs that penetrated through inserts (Fig. 2b). These results highlight the importance of HA in promoting transport of HA-SNP through the cells.

Spheroids are another attractive 3D tumor model.[26, 27, 29] It is established that tumor spheroids 200–500 μm in diameter, but not smaller ones, develop the oxygen, nutrients, and energy gradients similar to those found *in vivo*.[32] Furthermore, in ovarian cancer, spheroid formation has been associated with more invasive phenotype and higher resistance to chemotherapeutics *in vivo*.[33] To prepare SKOV-3 spheroids, we exploited a modified hanging drop method.[34] Incubating SKOV-3 cells in a hanging drop for 10 days generated flat, disc-like aggregates as determined by light microscopy (Fig. 3a) and confirmed by SEM (Fig. 3b). Transferring the flat aggregates to the adhesion resistant agarose surface caused

them to fold (Fig. 3c) and grow into spherical, compact 3D spheroids with diameters of 250–350 μm after 7 days (Fig. 3d and Fig. S3). The cells in the spheroids were mostly viable as determined by a LIVE/DEAD assay using the Calcein AM dye to mark live cells and the red ethidium homodimer to label dead cells (Fig. 3e).

The SKOV-3 spheroids were incubated with the SNPs and HA-SNPs respectively and unbound particles were washed off. After incubation, the number of cells labeled with NPs was quantified by flow cytometry with HA-SNPs leading to a 4.5 fold increase in the number of cells being labeled compared with the SNPs (Fig. 4a). When the spheroids were incubated with HA-SNP in the presence of HA polymer, the uptake of the NPs was reduced by 45% (Fig. 4b), demonstrating the HA-dependent nature of the uptake. Z-stack confocal microscopy images of the spheroids after incubation were acquired (Fig. 4c,d). While the SNPs exhibited little penetration (Fig. 4c), HA-SNPs were found deep into the spheroids (Fig. 4d). These observations correlate well with MCC penetration results and suggest the potential application of HA-SNPs as a drug delivery vehicle that can access cells in the interior of the tumor.

3.2. Toxicity enhancement of DOX delivered by HA-SNPs to 3D ovarian cancer spheroids

Having validated the HA-dependence for enhanced NP uptake and penetration, we studied DOX delivery by HA-SNP. SKOV-3 cells were loaded with DOX-HA-SNP at sub-toxic levels. After washing off unbound NPs, the loaded cells were incubated in culture media. Analysis of the culture media showed that the fluorescence intensities of both FITC and DOX went up over time, suggesting at least some DOX was still retained on HA-SNP after the internalized NPs were exported.

Next, we tested whether HA-SNP can enhance the penetration of DOX using the SKOV-3 MCC. DOX-HA-SNP or free DOX was added to the chamber above MCC respectively at the same sub-toxic DOX concentrations. The TEER measurements showed no electrical resistance changes over 24 hours indicating DOX did not affect the tight junctions much at the concentrations used. The DOX fluorescence intensities of the bottom chambers were measured after 24 hour incubation. With DOX-HA-SNP, the amount of DOX fluorescence in the bottom chamber was more than three times higher than that with free DOX (Fig. S4), suggesting that HA-SNP can significantly improve tumor penetration ability of DOX.

To analyze the cytotoxicity of DOX-HA-SNP, the SKOV-3 spheroids were incubated with DOX-HA-SNP as well as free DOX for 72 hours after which the spheroids were collected and dissociated. The numbers of live and dead cells were determined by a trypan blue exclusion assay. In this assay, dead cells were stained blue by the trypan blue dye since their membranes were compromised, while live cells excluded the trypan blue dye from entering thus remaining colorless. For free DOX, 13.2 μM of DOX was needed to kill 50% of the SKOV-3 cells in the spheroid (IC_{50} = 13.2 μM) (Fig. 5). In comparison, DOX-HA-SNPs exhibited 10-fold enhancement in cytotoxicity with an IC_{50} value of 1.3 μM. The HA-SNPs were not toxic to SKOV-3 cells as the cells retained 100% viability when treated with HA-SNPs (1.3 mg NP/mL).

The morphologies of the spheroids after drug treatment were examined by SEM and confocal microscopy. At a DOX concentration of 3.5 μM, free DOX did not have a significant effect on spheroid integrity. The DOX-free HA-SNPs did not influence the morphology of the spheroids either. In contrast, incubation with DOX-HA-SNPs at the equivalent DOX concentration of 3.5 μM disintegrated the spheroids causing severe deformations of their architecture (Fig. 6a). The effect was more pronounced at 20 μM of DOX-HA-SNPs (Fig. 6b vs 6c, 6d). Confocal images of the spheroids showed extensive distribution of DOX fluorescence throughout the spheroid (Fig. 6e), which overlaid well

with the green fluorescence from the SNP core (Fig. 6f,g). The SKOV-3 cells were also imaged under higher magnification upon DOX-HA-SNP incubation (Fig. 6h–k). Extensive red fluorescence of DOX was observed in the cytoplasm signaling significant intracellular DOX accumulation (Fig. 6j).

Multi-drug resistance is a major obstacle for effective cancer therapy.[35, 36] To test the effect of DOX-HA-SNP on resistant cancer cells, spheroids consisted of the multi-drug resistant NCI/ADR-RES ovarian cancer cells[37] were prepared (Fig. 7a–c) using a similar protocol as that for SKOV-3 cells. CD44 has been identified as a surface biomarker on NCI/ADR-RES cells,[38] which can serve as a potential therapeutic target to overcome drug resistance.[39] Confocal microscopy imaging confirmed that HA-SNPs penetrated deep into the NCI/ADR-RES spheroids than the SNPs (Fig. S5). The cytotoxicity of DOX-HA-SNPs to NCI/ADR-RES spheroids was evaluated using the trypan blue exclusion assay (Fig. 7g). Compared to free DOX (IC_{50} = 100 μM), DOX-HA-SNPs displayed significant enhancement in potency (IC_{50} = 20 μM). SEM images collected for NCI/ADR-RES spheroids treated with 20 μM DOX equivalent of DOX-HA-SNP showed the formation of holes and signs of spheroid disintegration (Fig. 7e,f), while at the same concentration, free DOX had little effect (Fig. 7d).

4. Conclusions

We demonstrated that HA coating significantly enhanced tumor penetration abilities of SNPs, presumably through CD44 mediated endocytosis followed by NP exocytosis. When evaluated in 3D tumor models, HA-SNPs enabled NP delivery to larger number of cells inside the tumor spheroids. DOX delivered by HA-SNPs were more potent against not only drug sensitive but also drug resistant ovarian cancer cells compared to free DOX. During the course of our work, two other reports utilizing receptor mediated transcytosis to enhance NP penetration of tumor have been published.[20, 25] Li and coworkers discovered that by immobilizing an agonist towards the melanocortin type-1 receptor on melanoma cells, the targeting gold NPs exhibited much wider dispersion in melanoma tissue through transcellular transport compared to the non-targeted counterparts.[20] The Fang group took advantage of the integrin-mediated transcytosis process to enhance the permeation of paclitaxel coated NP into solid tumor with greater tumor growth inhibitory effects.[25] Therefore, it may be general that by targeting a receptor such as CD44, which can undergo recycling between cell surface and endosomes/lysosomes and mediate transcytosis, tumor penetration by NPs can be significantly enhanced. This represents a promising new direction to improve the efficacy of the chemotherapeutic agent delivered by NPs for anti-tumor therapy.

Supplementary Material

Refer to Web version on PubMed Central for supplementary material.

Acknowledgments

This work was supported by NIH (R01CA149451) and an NSF CAREER award.

References

1. Minchinton AI, Tannock IF. Nature Rev. Cancer. 2006; 6:583–592. [PubMed: 16862189]
2. Tannock IF, Lee CM, Tunggal JK, Cowan DSM, Egorin MJ. Clin. Cancer Res. 2002; 8:878–884. [PubMed: 11895922]

3. Sugahara KN, Teesalu T, Karmali PP, Kotamraju VR, Agemy L, Greenwald DR, Ruoslahti E. Science. 2010; 328:1031–1035. [PubMed: 20378772]
4. Teesalu T, Sugahara KN, Kotamraju VR, Ruoslahti E. Proc. Natl. Acad. Sci. USA. 2009; 106:16157–16162. [PubMed: 19805273]
5. Goodman TT, Olive PL, Pun SH. Int. J. Nanomed. 2007; 2:265–274.
6. Kong SD, Zhang W, Lee JH, Brammer K, Lal R, Karin M, Jin S. Nano Lett. 2010; 10:5088–5092.
7. Huang K, Ma H, Liu J, Huo S, Kumar A, Wei T, Zhang X, Jin S, Gan Y, Wang PC, He S, Zhang X, Liang X-J. ACS Nano. 2012; 6:4483–4493. [PubMed: 22540892]
8. Tong R, Hemmati HD, Langer R, Kohane DS. J. Am. Chem. Soc. 2012; 134:8848–8855. [PubMed: 22385538]
9. Wong C, Stylianopoulos T, Cui J, Martin J, Chauhan VP, Jiang W, Popović Z, Jain R, Bawendi MG, Fukumura D. Proc. Natl. Acad. Sci. USA. 2011; 108:2426–2431. [PubMed: 21245339]
10. El-Dakdouki MH, Puré E, Huang X. Nanoscale. 2013 submitted.
11. Tammi R, Rilla K, Pienimaki JP, MacCallum DK, Hogg M, Luukkonen M, Hascall VC, Tammi M. J. Biol. Chem. 2001; 276:35111–35122. [PubMed: 11451952]
12. Ouasti S, Kingham PJ, Terenghi G, Tirelli N. Biomaterials. 2012; 33:1120–1134. [PubMed: 22071098]
13. Petros RA, DeSimone JM. Nature Rev. Drug Disc. 2010; 9:615–627.
14. Zhang S, Li J, Lykotrafitis G, Bao G, Suresh S. Adv. Mater. 2009; 21:419–424. [PubMed: 19606281]
15. Bareford LM, Swaan PW. Adv. Drug Del. Rev. 2007; 59:748–758.
16. Jiang X, Röcker C, Hafner M, Brandholt S, Dörlich RM, Nienhaus GU. ACS Nano. 2010; 4:6787–6797. [PubMed: 21028844]
17. Qiao R, Jia Q, Hüwel S, Xia R, Liu T, Gao F, Galla HJ, Gao M. ACS Nano. 2012; 6:3304–3310. [PubMed: 22443607]
18. Slowing II, Vivero-Escoto JL, Zhao Y, Kandel K, Peeraphatdit C, Trewyn BG, Lin VS-Y. Small. 2011; 11:1526–1532. [PubMed: 21520497]
19. Jin H, Heller DA, Strano MS. Nano Lett. 2008; 8:1577–1585. [PubMed: 18491944]
20. Lu W, Xiong C, Zhang R, Shi L, Huang M, Zhang G, Song S, Huang Q, Liu G-Y, Li C. J. Control. Release. 2012; 161:959–966. [PubMed: 22617522]
21. Nam J, Won N, Jin H, Chung H, Kim S. J. Am. Chem. Soc. 2009; 131:13639–13645. [PubMed: 19772360]
22. Stojanov K, Georgieva JV, Brinkhuis RP, van Hest JC, Rutjes FP, Dierckx RAJO, de Vries EFJ, Zuhorn IS. Mol. Pharmaceutics. 2012; 9:1620–1627.
23. Dombu CY, Kuroubi M, Zibouche R, Matran R, Betbeder D. Nanotech. 2010; 21:355102.
24. Panyam J, Labhasetwar V. Pharm. Res. 2003; 20:212–220. [PubMed: 12636159]
25. Jiang X, Xin H, Gu J, Xu X, Xia W, Chen S, Xie Y, Chen L, Chen Y, Sha X, Fang X. Biomaterials. 2013; 34:1739–1746. [PubMed: 23211449]
26. Hirschhaeuser F, Menne H, Dittfeld C, West J, Mueller-Klieser W, Kunz-Schughart LA. J. Biotechnol. 2010; 148:3–15. [PubMed: 20097238]
27. Goodman TT, Ng CP, Pun SH. Bioconjugate Chem. 2008; 19:1951–1959.
28. Padrón JM, van der Wilt CL, Smid K, Smitskamp-Wilms E, Backus HH, Pizao PE, Giaccone G, Peters GJ. Crit. Rev. Oncol. Hematol. 2000; 36:141–157. [PubMed: 11033303]
29. Ho WJ, Pham EA, Kim JW, Ng CW, Kim JH, Kamei DT, Wu BM. Cancer Sci. 2010; 101:2637–2643. [PubMed: 20849469]
30. Heldin C-H, Rubin K, Pietras K, Oestman A. Nat. Rev. Cancer. 2004; 4:806–813. [PubMed: 15510161]
31. Cowan DS, Hicks KO, Wilson WR. Br. J. Cancer. 1996; 27:S28–S31.
32. Friedrich J, Seidel C, Ebner R, Kunz-Schughart LA. Nat. Protoc. 2009; 4:309–324. [PubMed: 19214182]
33. Sodek KL, Ringuette MJ, Brown TJ. Int. J. Cancer. 2009; 124:2060–2070. [PubMed: 19132753]

34. Kelm JM, Timmins NE, Brown CJ, Fussenegger M, Nielsen LK. Biotechnol. Bioeng. 2003; 83:173–180. [PubMed: 12768623]
35. Szakács G, Paterson JK, Ludwig JA, Booth-Genthe C, Gottesman MM. Nat. Rev. Drug Discov. 2006; 5:219–234. [PubMed: 16518375]
36. Perez-Tomas R. Curr. Med. Chem. 2006; 13:1859–1876. [PubMed: 16842198]
37. Liscovitch M, Ravid D. Cancer Lett. 2007; 245:350–352. [PubMed: 16504380]
38. Cain JW, Hauptschein RS, Stewart JK, Bagci T, Sahagian GG, Jay DG. Mol. Cancer Res. 2011; 9:637–647. [PubMed: 21357442]
39. Misra S, Ghatak S, Toole BP. J. Biol. Chem. 2005; 280:20310–20315. [PubMed: 15784621]

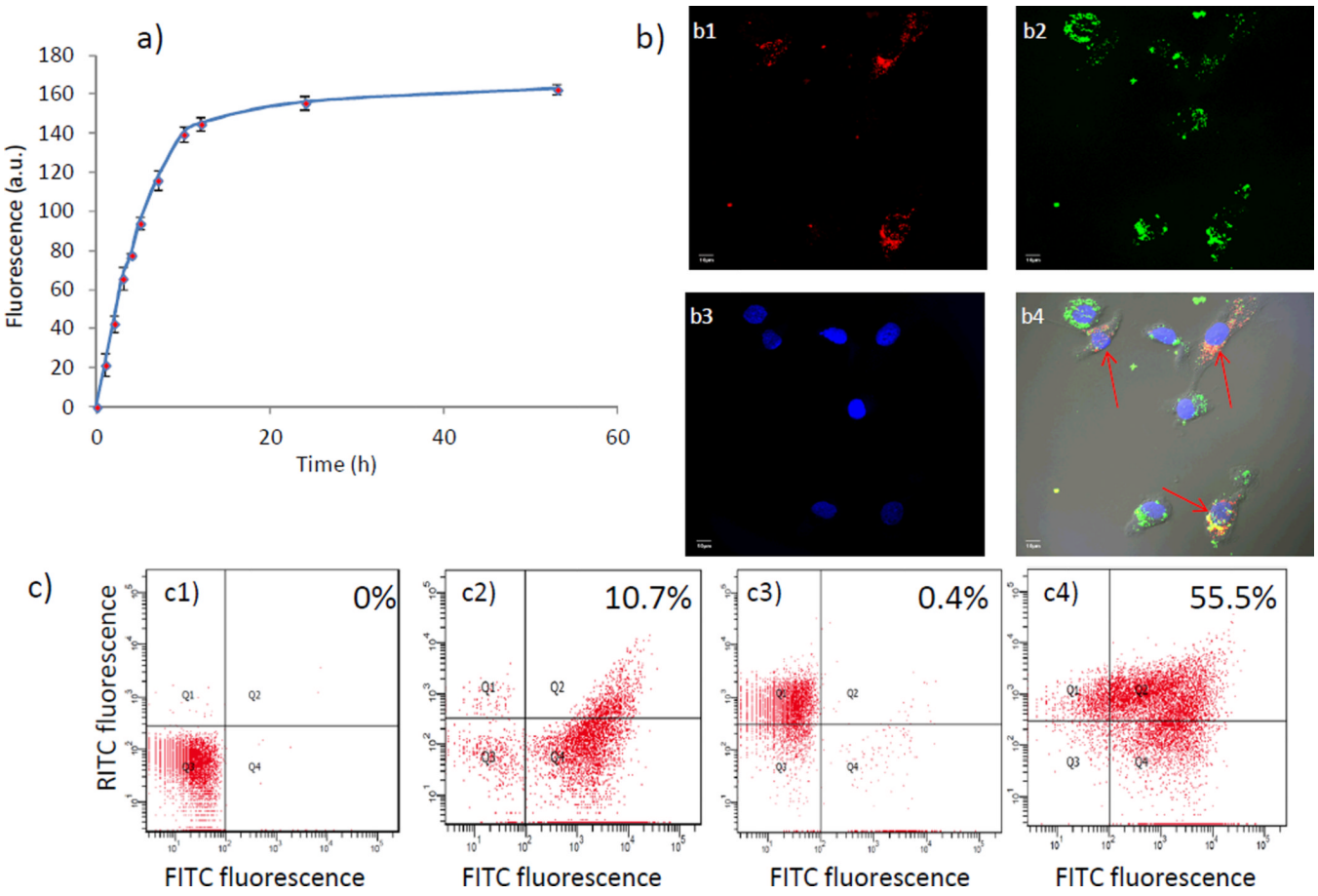

Fig. 1.

(a) Time dependent release of HA-SNPs from SKOV-3 cells showing that the internalized HA-SNPs can be exported. (b) Confocal images of SKOV-3 cells in the two particle assay. b1, RITC channel showing location of HA-RITC-SNP; b2, FITC channel showing location of HA-SNP; b3, DAPI channel showing location of the nucleus; b4, overlay of RITC, FITC, DAPI channels and DIC images. The scale bars are 10 μm. In this experiment, cells were pre-loaded with either the green fluorescent HA-SNPs or the red fluorescent HA-RITC-SNPs. The pre-loaded cells were then cultured together. Some cells (marked with red arrows) exhibited both green and red fluorescence indicating that exocytosed NPs could be taken up by cells. (c) Quantification of double labeled cells by flow cytometry. c1) control unlabeled cells; c2) cells incubated with HA-SNP only; c3) cells incubated with HA-RITC-SNP only; c4) co-incubation of cells pre-loaded with HA-SNPs or HA-RITC-SNP for 48 h led to 55.5% of cells giving high fluorescence for both FITC and RITC indicating that the exocytosed SNPs can be efficiently internalized by other cells.

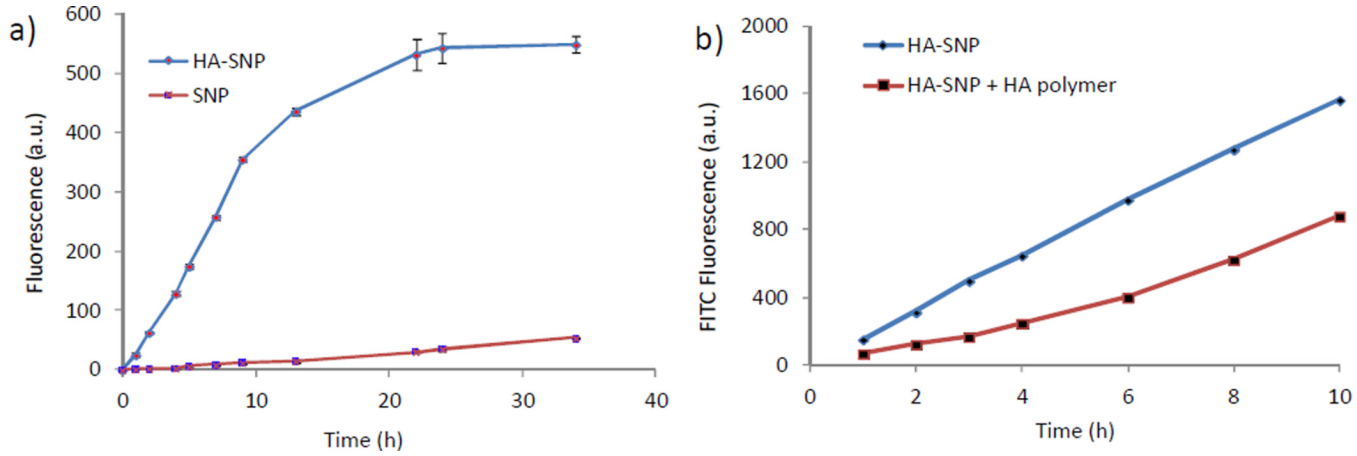

Figure 2.

a) Penetration of NPs through MCC. HA-SNPs showed significantly enhanced penetration abilities compared to the control SNPs. b) Penetration of HA-SNPs through MCC in the absence (blue) and presence of free HA polymer (red). HA polymer was added 2 h prior to addition of HA-SNP. HA polymer reduced the amount of HA-SNP that penetrated through MCC.

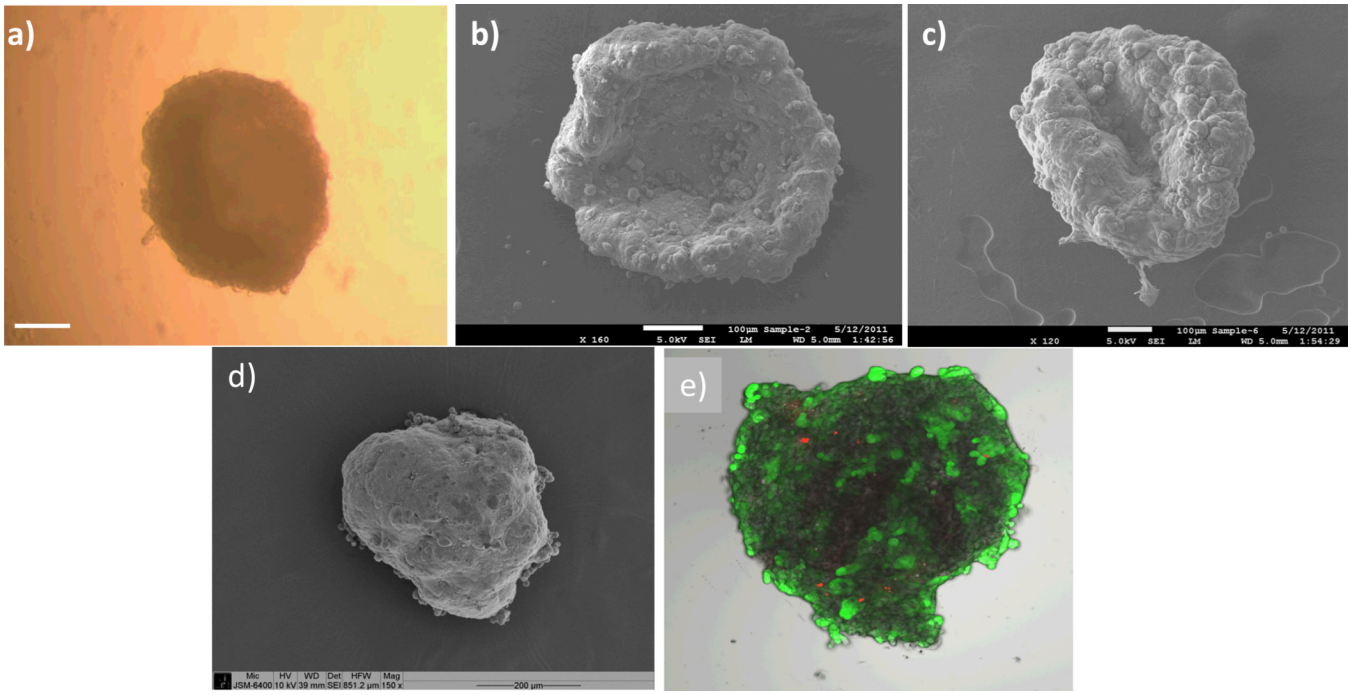

Fig. 3.

3D SKOV-3 spheroids formed by the hanging drop method. (a) A 2D Light microscope image and (b) a SEM image of a spheroid grown by the hanging drop method *without* being transferred to an agarose-coated surface. (c) SEM image of a spheroid grown using the hanging drop method and transferred to an agarose-coated surface. The image showed the folding and the growth of the spheroid after growing on the agarose surface for 4 days. (d) SEM and (e) viability of fully grown SKOV-3 spheroids after growing on the agarose surface for 7 days (the green color from Calcein marks live cells and the red color from ethidium homodimer marks dead cells). The scale bars are 200 μm (a, d) and 100 μm (b, c).

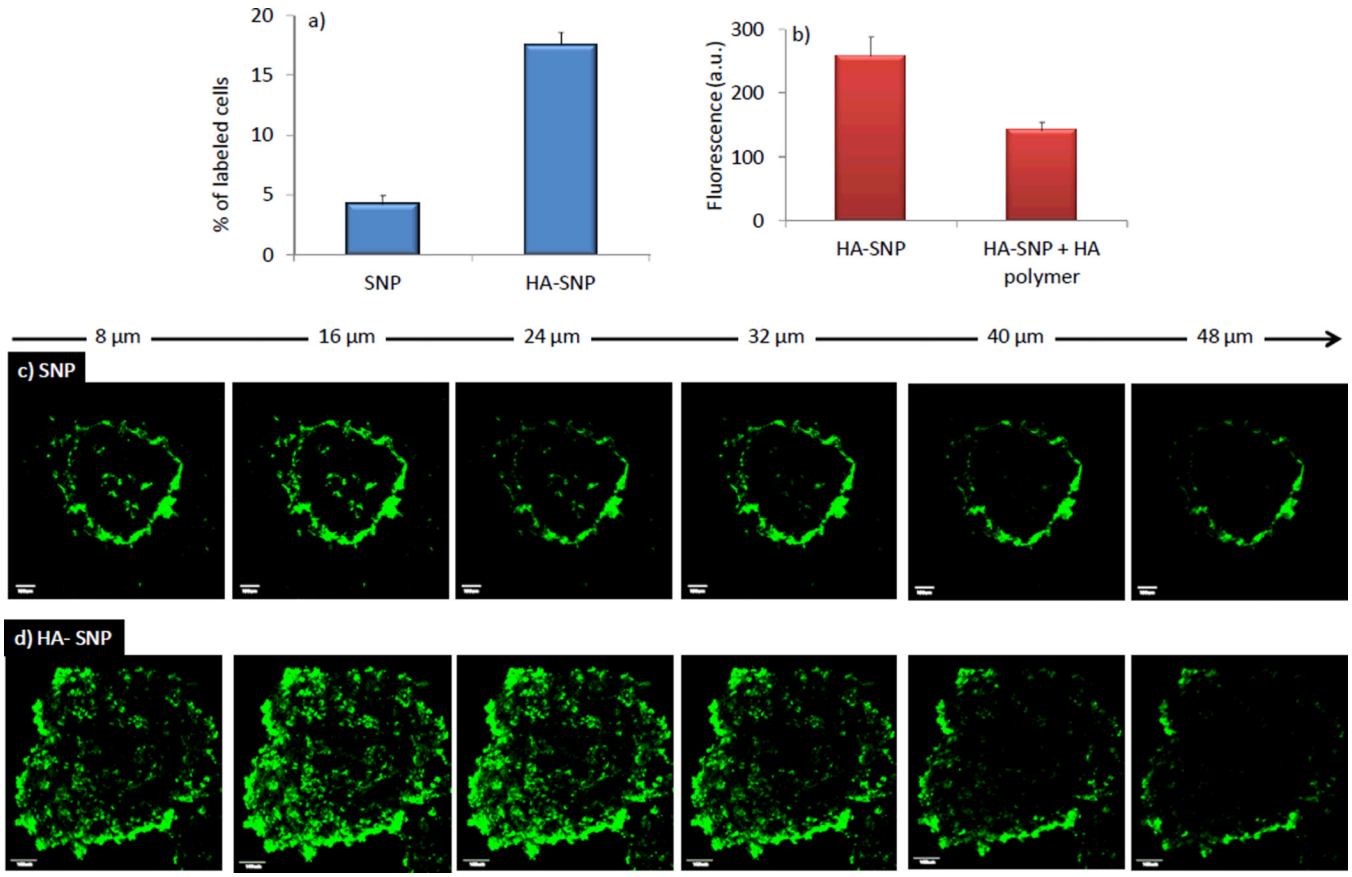

Fig. 4.

a) Percentage of cells labeled with NPs in SKOV-3 spheroids after incubating the spheroids with SNPs or HA-SNPs respectively for 6 hours. b) Uptake of HA-SNPs by spheroids in the presence and absence of free HA polymer. Z-stake confocal images of spheroids incubated with c) SNPs and d) HA-SNPs after incubation. SNPs displayed poor penetration power and were mainly bound to the exterior of the spheroid. In contrast, HA-SNPs penetrated much deeper into the spheroid. The scale bar is 100 µm.

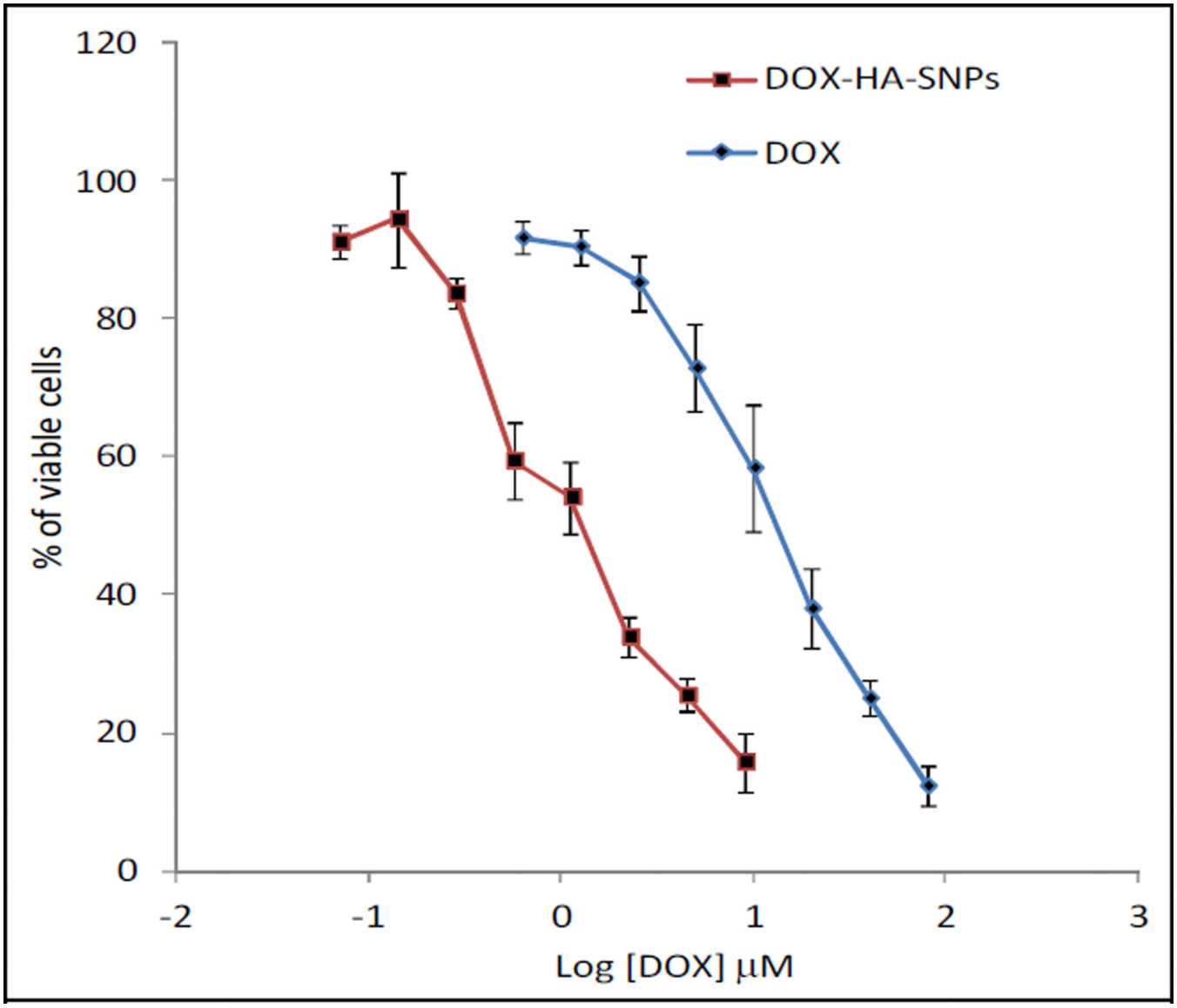

Fig. 5.
Trypan blue exclusion assay showing the cytotoxicity of DOX and DOX-HA-SNPs against SKOV-3 spheroids. The DOX-HA-SNPs were more cytotoxic than free DOX.

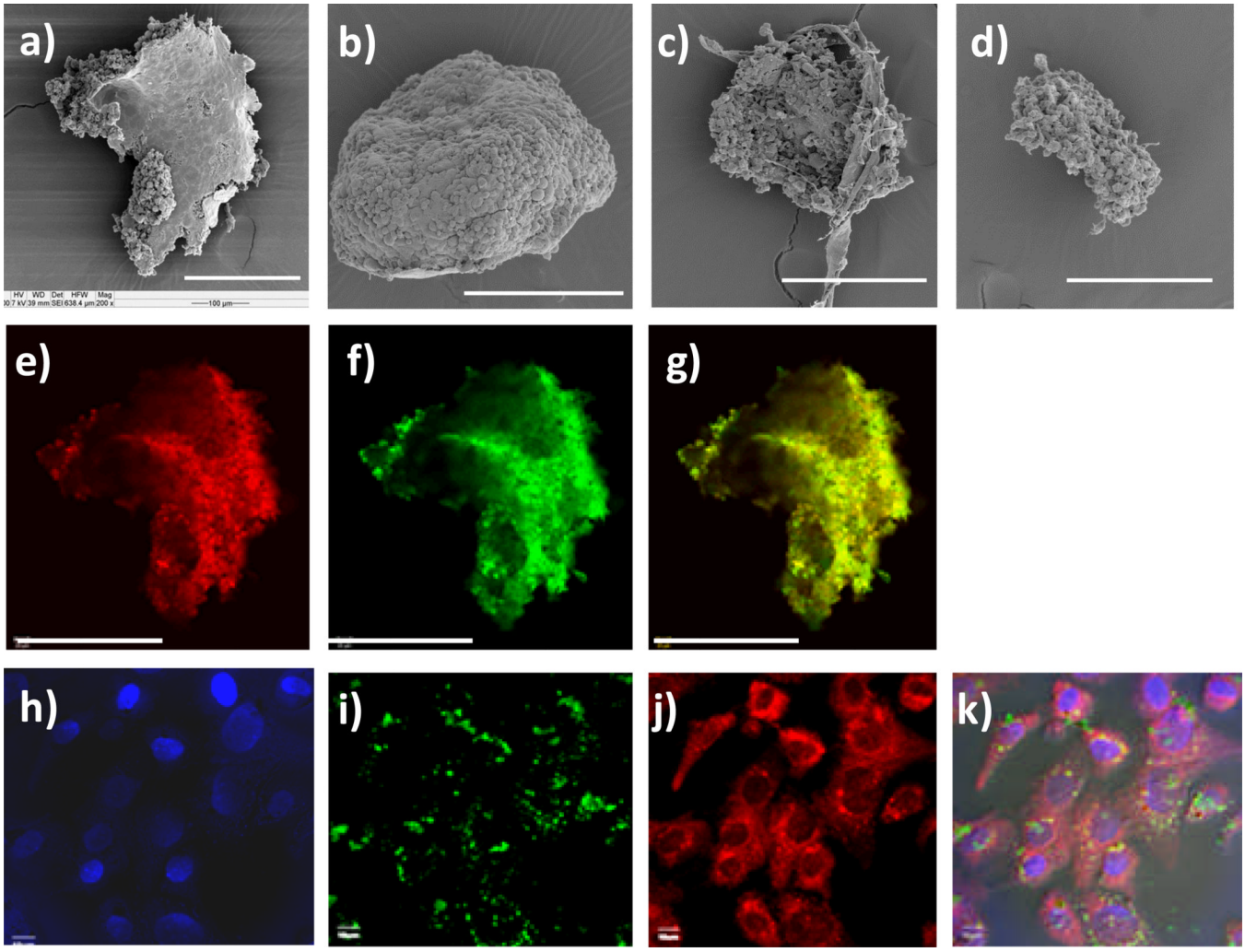

Fig. 6.

SEM images of a) a SKOV-3 spheroid treated with DOX-HA-SNP (equivalent to 3.5 μM of DOX) for 72 h showing disintegration of the spheroid; SKOV-3 spheroids treated with (b) DOX or (c, d) DOX-HA-NP at [DOX]= 20 μM. The DOX-HA-NP caused major reduction in the size and profound deformation of the spheroids, while free DOX did not have significant effects on spheroids at the concentrations tested. Confocal images of the spheroid shown in (a): e) DOX channel, f) FITC channel, and (g) is overlay of (e) and (f). The scale bars in a–g) are 200 μm. h–k) Confocal images of SKOV-3 cells upon incubation with DOX-HA-SNP. h) DAPI channel showing positions of the nuclei; i) FITC channel showing NP locations; j) DOX channel showing location of DOX; and k) overlay of images in h)–j) and the DIC images. The scale bars in h–k) are 10 μm.

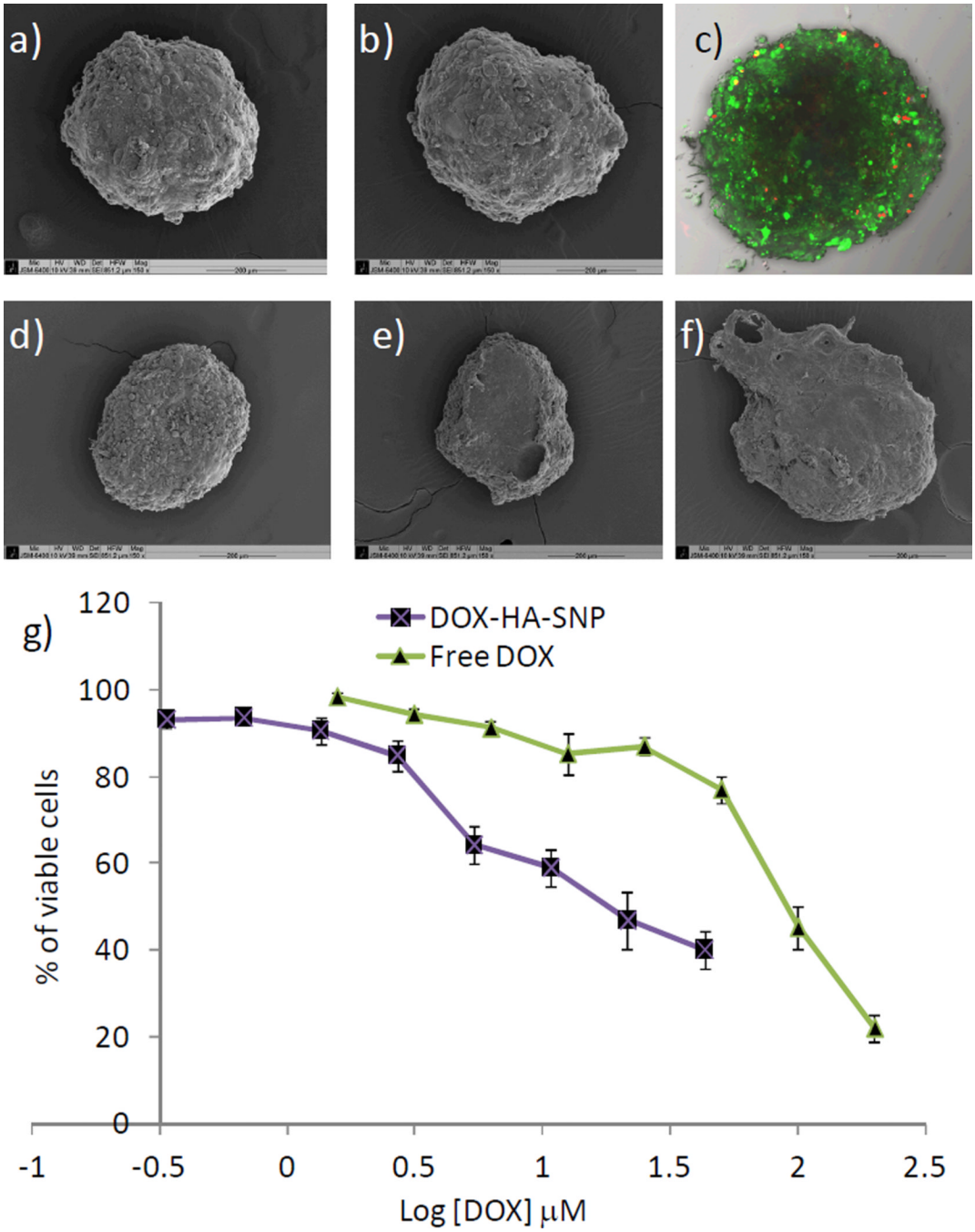

Fig. 7.

(a) and (b) show the SEM images of two representative NCI/ADR-RES spheroids prepared by the modified hanging drop method. (c) shows LIVE/DEAD assay to demonstrate the viability of NCI/ADR-RES spheroids (the green color from Calcein marks live cells and the red color from ethidium homodimer marks dead cells). The scale bar is 200 μm. (d, e, f) SEM images of NCI/ADR-RES spheroids treated with (d) DOX or (e, f) DOX-HA-NP at [DOX]= 20 μM. The NP formulation caused thinning and the formation of holes the NCI/ADR-RES spheroids. (g) Trypan blue exclusion assay showing the cytotoxicity of DOX and DOX-HA-SNPs against NCI/ADR-RES spheroids. The DOX-HA-SNPs were more cytotoxic than free DOX.